http://www.sciencedirect.com/science/article/pii/S2352409X15300353

DOI: 10.1016/j.jasrep.2015.06.016

(http://dx.doi.org/10.1016/j.jasrep.2015.06.016)

CENTRAL MEDITERRANEAN PHOENICIAN POTTERY IMPORTS IN THE NORTHEASTERN IBERIAN PENINSULA

E. Miguel Gascón, J. Buxeda i Garrigós, P. M. Day

Journal of Archaeological Science: Reports, 3, 237–246 (2015)

CENTRAL MEDITERRANEAN PHOENICIAN POTTERY IMPORTS IN THE NORTHEASTERN IBERIAN PENINSULA

Eva Miguel Gascón*[1], Jaume Buxeda i Garrigós[1] and Peter M. Day[2]

[1]Cultura Material i Arqueometria UB (ARQUB, GRACPE), Dept. de Prehistòria, Història Antiga i Arqueologia, Universitat de Barcelona, Montalegre 6, 08001 Barcelona, Catalonia, Spain

[2] Department of Archaeology, University of Sheffield, Northgate House, West Street, Sheffield S1 4ET, United Kingdom

Corresponding author. Tel.: +34 685532585

E-mail addresses: evamigascon@gmail.com (E. Miguel Gascón), jbuxeda@ub.edu (J. Buxeda i Garrigós), p.m.day@sheffield.ac.uk (P. M. Day).

ABSTRACT

Over recent years, there has been a growing interest in the analytical investigation of Phoenician pottery recovered from sites in Catalonia (NE Iberian Peninsula). Studies which integrate mineralogical, chemical and microstructural analysis have been carried out at seven sites in the Ilercavonia and Cossetania areas, analyzing a total of 123 ceramic samples. The characterization of these samples has confirmed the presence of Phoenician Central Mediterranean pottery, all in the form of tableware.

The main objectives of this paper are to determine the provenance of these products, to study their mineralogical characteristics and to understand the consumption of this Phoenician Central Mediterranean pottery in the context of the sites of Ilercavonia and Cossetania.

All individuals have been analyzed by means of X-ray fluorescence (XRF) and X-ray diffraction (XRD), with selected samples analyzed by means of thin-section petrography and scanning electron microscopy (SEM). The results of this study demonstrate the presence of Sicilian, Sardinian and Tunisian products, allowing us to see preferences of vessel types according to source.

KEYWORDS: Iron Age; Phoenician commerce; X-ray fluorescence; X-ray diffraction; thin-section petrography; scanning electron microscopy

1. INTRODUCTION

Since 2002, analyses have been performed at the Universitat de Barcelona on the first wheel-thrown pottery found in indigenous contexts of the VIII century – 575 BC in the regions of Ilercavonia and Cossetania (Catalonia). Traditionally, this pottery has been thought to have been manufactured by potters located in a variety of Western Phoenician colonies.

Most of this pottery comprises amphorae whose provenance has been associated with the Circle of the Strait of Gibraltar, where the ancient Phoenician colonies (Aubet, 2009) of the Iberian Peninsula and Atlantic Sea were located (Figure 1). In the last years, a complex Phoenician cabotage system has been suggested (Rafel, 2013), starting from these Southern Andalucian sites, reaching along the Iberian Peninsula coast to the indigenous communities situated in Catalonia. This contact seems to have been commercial in nature, since there are no Phoenican colonies in the Ilercavonia and Cossetania regions. In fact, it is in the province of Málaga in Andalucia where intense archaeological work has revealed an extensive list of Phoenician sites, settlements and production centers (Toscanos, Cerro del Villar, La Pancha, Los Algarrobeños, Chorreras, Morro de Mezquitilla) and most studies of Phoenician pottery found in Catalonia point to this area as its source (Garcia and Gracia, 2011). However, amongst the Phoenician pottery found in the Cossetania and Ilercavonia regions of Catalonia, a small group, mainly tableware, is not related to a source area of the Circle of the Strait of Gibraltar.

Macroscopic study has proved of limited value in ascribing provenance to these vessels. As a result one of the main objectives of the analytical research reported here is to define the different Central Mediterranean Phoenician products detected at three sites in Northeast Iberia (Figure 2): Sant Jaume – Mas d'en Serrà, La Ferradura (Ilercavonia) and Turó de la Font de la Canya (Cossetania). In this paper we present some of the results of Miguel Gascón's unpublished Doctoral Thesis (Miguel Gascón, 2014).

The site of Sant Jaume - Mas d'en Serrà (Garcia and Gracia, 2011) has different types of pottery related to Central Mediterranean production. There are three narrow-necked cylindrical jars (MOS026, MOS040 and MOS060) and a carinated red slipped bowl (MOS037). The settlement features a defensive system unique in the whole of the Northeastern Iberian Peninsula during the Early Iron Age (Garcia, 2009). It seems that in Catalonia, Sant Jaume was one of the centres with the strongest trade relations with the Phoenician world, thus up to 30% of the wheel-made pottery excavated is related to Phoenician imports (Garcia *et al.,* 2015).

The other Ilercavonian site included in this study is La Ferradura (Maluquer, 1983), where only one indeterminate pot was related to a Central Mediterranean provenance (FER005). The settlement hosts a complex of eleven rooms, some clearly related to metallurgical activity. Most

Iron Age sites of Ilercavonia are related to metallurgy, which seems to be closely connected with Phoenician commerce.

In the case of Turó de la Font de la Canya (Asensio *et al.*, 2005), four narrow-necked cylindrical jars (TFC025, TFC036, TFC040, and TFC041) and one oil bottle (TFC072), were identified as Central Mediterranean products. This site is a *campo de silos*, a large area full of silos devoted to the storage of the product of a system of intense cereal exploitation. This type of settlement is predominant in the Cossetania region.

2. METHODS

2.1 X-ray fluorescence (XRF)

To characterize the chemical composition of these samples (Table 1), XRF was carried out in the Centres Científics i Tecnològics of the Universitat de Barcelona. Due to the long duration of the research project, two different XRF instruments were used. More detail information about the analytical routine has been published elsewhere (Miguel Gascón and Buxeda i Garrigós, 2013).

First, in the case of samples MOS026, MOS037 and MOS040, major and minor elements (MgO, Al_2O_3, SiO_2, P_2O_5, K_2O, CaO, TiO_2, MnO, and Fe_2O_3 -as total Fe-) were determined by preparing duplicates of glass beads. Trace elements (V, Cr, Co, Ni, Cu, Zn, Ga, Rb, Sr, Y, Zr, Nb, Mo, Sn, Ba, Ce, W, Pb, and Th), as well as Na_2O, were determined by powdered pills. The quantification of the concentrations was performed using a (WDXRF) Phillips PW2400 spectrometer with an Rh excitation source.

Samples MOS060, FER005, TFC025, TFC036, TFC040, TFC041 and TFC072 were analyzed with a different XRF machine. In this case, major and minor elements (including Na_2O) were determined by duplicates of glass beads. Trace elements were also determined by powdered pills. However, this time determination of concentrations was performed using an Axios^{mAX}-Advanced PANalytical spectrometer with an Rh excitation source.

All differences between the two XRF machines were taken into account in order to be able to compare the data obtained.

2.2 X-ray diffraction (XRD)

The mineralogical composition was studied by means of XRD at the Centres Científics i Tecnològics of the Universitat de Barcelona.

Measurements for samples MOS026, MOS037 and MOS040 were made using a Siemens D-500 diffractometer working with the Cu-Kα radiation (λ = 1.5406 Å) at 1.2 kW (45 kV – 30 mA). Measurements where taken from (4 to 70)º2θ, at 1°2θ min^{-1} (step size = 0.05°2θ; time = 3 s).

In the case of samples MOS060, FER005, TFC025, TFC036, TFC040, TFC041 and TFC072 measurements were made using a Bragg-Brentano PANalytical X'Pert PRO MPD Alpha diffractometer equipped with an X'Celerator detector, working with the Cu-Kα radiation (λ = 1.5406 Å) at 1.8 kW (45 kV – 40 mA). Measurements where taken from (4 to 100)º2θ, with an step size of 0.026°2θ and an acquisition time of 50 s per step.

2.3 Thin-section petrography

Samples MOS037, MOS040, FER005, TFC025, TFC036, and TFC041 were also analyzed in terms of thin-section petrography at the University of Sheffield. All specimens were cut transversely to the direction of the wheel-thrown marks using an Evans saw. Thin-sections were examined at a range of magnifications from x25 to x100 under a petrological microscope to study their mineralogy, petrography and texture. Petrographic groups were described following Whitbread's system (Whitbread, 1989, 1995).

2.4 Scanning electron microscopy (SEM)

Finally, some specimens (TFC041, TFC036 and MOS037) were selected for analysis by SEM attached to an energy-dispersive X-ray analyser (EDX) in order to characterize the microstructure, the sintering stage of the ceramic matrix and to identify aplastic inclusions. Thus, fresh fractures of the observed samples were coated with a carbon layer in a high vacuum atmosphere. An acceleration voltage of 20 kV, beam current of 1 nA, and 100 s per microanalysis was used.

These analysis were carried out at the Centres Científics i Tecnològics of the Universitat de Barcelona, using a *JEOL* JSM-6510 and Quanta 200 microscopes.

3. RESULTS

The elemental concentrations determined by means of XRF are a special case of the projective d+1-dimensional space, the simplex S^d. Projective points are represented by a d+1-dimensional vector of coordinates adding up to a constant k ($k \in R^+$),

$$\mathbf{x} = [x_1,..., x_{d+1}] \mid x_i \geq 0 \ (i = 1,..., d + 1), \ x_1 + \ldots + x_{d+1} = k,$$

(in the present case, k = 100), a subset in the positive orthant R^{d+1}, following a multiplicative model with logarithmic interval metrics (Barceló-Vidal *et al.*, 2001; Aitchison, 2005; Buxeda i Garrigós, 2008). Therefore, for the statistical data treatment, raw concentrations have been ALR (additive log-ratio) transformed, according to

$$\mathbf{x} \in S^{d} \rightarrow \mathbf{y} = \log\left(\frac{\mathbf{x}_{d}}{\mathrm{x}_{d+1}}\right) \in R^{d},$$

being S^d the d-dimensional simplex, $\mathbf{x}_{-D} = [x_1,...,x_d]$, and D = d+1, or CLR (centered log-ratio) transformed, according to

$$\mathbf{x} \in S^{d} \rightarrow \mathbf{z} = \log\left(\frac{\mathbf{x}}{g(\mathbf{x})}\right) \in R^{d+1},$$

being S^d the d-dimensional simplex, and g(**x**) the geometric mean of all D (D = d+1) components of **x** (Aitchison, 1986; Buxeda i Garrigós, 1999). Moreover, several elements were discarded: Mo and Sn due to low analytical precision, and Co and W because of the possible contaminations from the tungsten carbide cell of the mill. Th was also not taken into account, on account of possible interferences due to the high Sr concentrations, that could not be corrected in the case of those analysis done with the (WDXRF) Phillips PW2400 spectrometer.

A cluster analysis was performed with R software (R Core Team, 2013) using the square Euclidian distance and the centroid agglomerative algorithm on the subcomposition Na_2O, MgO, Al_2O_3, SiO_2, K_2O, CaO, TiO_2, MnO, and Fe_2O_3, with CLR transformation of the 218 Phoenician samples of the ARQUB's database (figure 3). Only major and minor elements were considered in this statistical treatment since the abovementioned dataset included 178 specimens analyzed by other research teams. These individuals belong to Phoenician pottery or to chronologically related ceramics, but only major and minor elements concentrations were determined. Moreover, since the analytical routine was also different from the present project and, in most cases, there are no inter-laboratory calibration studies, this comparison should be considered semi quantitative. The analytical case studies of these 178 specimens are: a study conducted at the Università di Palermo on the Phoenician productions of Mozia and Solunto in Sicily (Alaimo *et al.*, 1998, 2002); three studies conducted at the Insituto di Ricerche Technologiche per la Ceramica – CNR (Faenza) on the Phoenician tableware of Carthage (Amadori and Fabbri, 1998a), Toscanos (Amadori and Fabrri, 1998b), Sardinia (Tharros, Santo Antioco and Monte Sirai), and Ischia (Amadori and Fabbri, 1998c); the grey products from the Iberian site of Ullastret (Pradell *et al.*, 1995); the amphorae of the Palaià Polis of Empúries (Vendrell-Saz, 2005); and the Phoenician kilns of Cerro del Villar (Cardell *et al.*, 1999). In the case of Carthage, Sicily and Sardinia, control groups were formed by samples classified as local products on grounds of their typology, their chemical and mineralogical analysis by means of XRF and thin-section petrography.

The statistical data treatment is summarized in the dendrogram resulting from the cluster analysis in Figure 3. It shows a complex structure where we observe groups related to Central Mediterranean sources, according to the comparative data bank considered. Thus, group CER contains a possible Sardinian sample (MOS037), while a possible Sicilian provenance can be suggested for sample FER005, which is included in group SIC. Also of interest is a possible Tunisian (Carthaginian) provenance for samples TFC025, TFC036, TFC040, TFC041, TFC072, MOS026, MOS040 and MOS060 in the complex structure CAR that can be divided into four different groups: CARa, CARb, CARc and CARd.

Ther follows an assessment of the chemical and mineralogical data obtained through the XRF, XRD, SEM and petrographic analysis for each of these groups.

3.1 Carthaginian products: GR CARa, CARb, CARc and CARd

The compositional variation matrix enabled the quantification of the total variation (*vt*) present in the data matrix and the investigation of the source of this variability. In the case where all samples belonging to the CARa, CARb, CARc and CARd subgroups were considered as one group (CAR), *vt* has a high value (*vt* = 1.8). This suggests that these data have a polygenic character, which means that no all individuals exhibited similar compositions; so, following the provenance postulate, it would be expected that they represent different units of production (Buxeda i Garrigós and Kilikoglou, 2003). This chemical variability is linked to Ba, MnO, CaO, Na_2O, Th, Cu and Cr. The element that imposes the lowest relative variation is Al_2O_3 when used as divisor in ALR transformation and will, therefore, be used in the statistical data treatment (Buxeda i Garrigós, 1999). Because of the extreme variability introduced by Na_2O and Ba these elements excluded from the statistical data treatment. Also Pb, Cu and P_2O_5 were not used because they are known to be sensitive to post-depositional perturbations.

A cluster analysis was performed, using the Euclidian distance and the centroid agglomerative algorithm on the subcomposition MgO, SiO_2, K_2O, CaO, TiO_2, V, Cr, MnO, Fe_2O_3, Ni, Zn, Ga, Rb, Sr, Y, Zr, Nb, and Ce, ALR transformed using Al_2O_3 as divisor.

Figure 4 shows the dendrogram resultant from this statistical treatment. The first group that appears, CARa, includes individuals MOS040 and MOS060 that present the lowest CaO concentrations among the Tunisian groups (9.60%, table 2). Next to it, another group, CARb, with samples TFC025, TFC040 and TFC041 presents the highest concentrations in Rb (114 ppm, table 2). More separated appears CARc including a single individual, TFC072, which is the most calcareous specimen of the Carthaginian products analyzed (26.1% in normalized data, table 1 and table 2). Finally, CARd, presents the highest concentrations of Zn for samples TFC036 and MOS026 (94 ppm, table 2).

Petrographic analysis was performed on individuals MOS040 (CARa); TFC025, TFC041 (CARb); and TFC036 (CARd). It was possible to identify different petrographic groups:

Group 1. This group is represented by sample TFC036 (Figure 5), characterized by the presence of rounded quartz and calcite inclusions. There are very rare to rare voids forming an estimated <1% of the volume. Open-spaced common mesovughs, rare mesochannels and elongate voids, have a strong alignment to the vessel wall. Mostly equant aplastic inclusions exhibit a poor alignment parallel to the vessel wall.

It presents a fine, dense calcareous matrix homogeneous throughout the section. The colour is brown to greyish in PPL and dark brown in XP (x25). The micromass is optically inactive. The inclusions appear to have a bimodal grain-size distribution; the coarse fraction is set in a finer-grained groundmass. It is generally sub-rounded to well-rounded and well sorted. Micro fauna composed by foraminifera of *globigerinida* species are present in the coarse fraction. Calcite crystals have replaced the multi-chambered walls and, in very rare cases, they also contain iron oxide (size < 0.08 mm). This type of microfossil is also common in the fine fraction (size <0.04 mm, mode = 0.025 mm). The abundance of these microfossils and sandstone indicate a sedimentary environment.

Group 2. The dominant inclusion of this fabric consists of crushed calcite. It is represented by sample TFC025 (figure 6). Its microstructure presents very rare voids, with few mesovughs and very rare mesochannels. Elongate voids are open-spaced and display strong alignment to the margins of section with. Elongate and equant aplastic inclusions exhibit a moderate alignment to the vessel walls.

It features a fine calcareous matrix predominantly homogeneous throughout the section. It is brown/orange in PPL and brown/red in XP (x25) and optically very active. Crushed calcite is the dominant inclusion in coarse fraction, angular, euhedral and equant and well sorted (size <0.32 mm, mode = 0.15 mm).

Textural concentration features (Tcf) are bright red in PPL and dark red in XP (x25) with clear to merging boundaries and very high optical density. They are generally equant, rounded and have high sphericity, discordant with the micromass. The commonly display fine-grained monocrystalline quartz inclusions, with varying amounts of ferruginous matter, sometimes almost opaque. They are probably clay pellets (size 0.036 mm to 0.016 mm).

The angular and even regular shape of calcite inclusions present in this sample suggest that this mineral was crushed and added deliberately to the clay as temper.

Group 3. This is defined by allotriomorphic quartz and mica as predominant inclusions in the matrix (Sample MOS040 and TFC041, Figure 7). The microstructure shows rare to few voids, forming an estimated 1-3% of the volume. There are common meso- and microvughs and rare mesochannels. Elongate voids have a very strong alignment to the margins of sections and are single to double-spaced.These display partial infilling with secondary calcite. The equant, aplastic inclusions mostly exhibit a poor alignment to the vessel walls.

The predominantly fine calcareous and homogeneous is brown in PPL and dark orange/brown in XP (x25). The micromass is optically active, evident in MOS040, due to a low firing temperature.

Quartz (size < 0.032 mm, mode = 0.018 mm) and muscovite mica (size < 0.024 mm, mode = 0.015 mm) are frequent in the fine fraction. Calcite is common and there are few iron oxides and opaques. Rare foraminifera microfossils are present in TFC041.

There are two different types of Tcf in sample TFC041. The first is dark orange in PL and brown in XP (x25), with clear boundaries and is optically dense. This type is generally sub-angular, discordant with the micromass and contains non-plastic inclusions of fine, monocrystalline quartz and calcite crystals (size < 0.16 mm, possible clay pellets). Another Tcf, of dark red colour in PPL and XP (x25) most almost opaque, with clear, sharp boundaries. In some case there is a surrounding void. Optically it is extremely dense and sub-angular, discordant with the micromass, with non-plastic inclusion, such as fine-grained monocrystalline quartz, distinguishable (size = 0.3 mm, possible grog).

Microfossils are more abundant and larger in MOS040, in both the coarse and fine fraction It is also possible to distinguish foraminifera and crushed molluscs (size < 0.1 mm, mode = 0.05 mm). The rounded to well-rounded monocrystalline quartz fragments present in the matrix is a diagnostic feature to relate these samples with a desert environment. It may be suggested that TFC041 is a finer version of TFC025.

XRD results allow the identification of different fabrics (Buxeda *et al.*, 1995) within each chemical group of the Carthaginian products. In the case of group CARa there is just one fabric, CARa-I, represented by samples MOS040 and MOS060. It is possible to estimate a low equivalent firing temperature (EFT) below (800/850) ºC, since no firing phases were observed (Figure 8, top).

Again, only one fabric was defined for group CARb, comprising samples TFC025, TFC040 and TFC041 (CARb-I). Its EFT can be estimated below (800/850) ºC.

CARc contains only one sample, TFC072, (CARc-I). The diffractogram of this oil bottle (Figure 8, centre) presents quartz, gehlenite, calcite, plagioclase and analcime, which is a sodic zeolite that appears as a perturbation in high fired calcareous ceramics (Buxeda, 1999). Its EFT can be estimated around (1000/1050) ºC.

Two fabrics can be distinguished for CARd. Sample MOS026 represents fabric CARD-I with a low EFT, below (800/850) ºC. Fabric CARd-II is represented by sample TFC036 (Figure 8, bottom) with an EFT estimated c. (950/1000-1050) ºC. This EFT, similarly to the CARc-I fabric, is indicated by the total decomposition of illite-muscovite and the crystallization of plagioclase, pyroxene and gehelenite. Therefore, the presence of calcite must be associated with a secondary origin, as observed in petrographic analysis (Cau *et al*.,2002).

The study of these products was completed by SEM analysis. Fabric CARb-I was studied through sample TFC041 and it was possible to confirm its low firing (Figure 9, top), through its non vitrificatied (NV) matrix (Kilikoglou, 1994). The EFT could thus be below 750 ºC. Fabrics CARa-I, CARc-I and CARd-I were not analyzed. In fabric CARd-II a stage close to total vitrification (Vc+-TV) was observed (Figure 8) and its EFT can be estimated at around (1050-1080) ºC.

3.2 Sardinian production: GR CER

Sample MOS037 can be related to a Sardinian provenance. This red slip carinated bowl is grouped together with the reference groups of the Phoenician site of Sulcis (Acquaro, 1998; Amadori and Fabbri, 1998c). It presents high concentrations in Na_2O, K_2O, Rb, Y, and Ce (1.92%, 4.41%, 182 ppm, 46 ppm, and 121 ppm in normalized data, respectively, table 1).

Petrographic analysis characterized MOS037 as a different group, where Tcfs are the principal inclusion (Figure 10).

Group 4. There are rare to very few voids in this sample: common mesovughs, single to open spaced, elongate and with a strong alignment to the section margins. Elongate and equant aplastic inclusions exhibit moderate alignment parallel to the vessel walls.

The sample has a fine calcareous, largely homogeneous matrix, which is light brown to greyish-brown in PPL and orange-reddish to brown in XP (x25). Frequent Tcfs occur in both the coarse and fine fraction. They are dark red to opaque in PPL and brown-reddish to opaque in XP (x25), with sharp to clear boundaries and very high optical density. They are usually angular to sub-angular and discordant with the micromass. Some have monocrystalline quartz and calcite inclusions similar to those in the matrix. Their angularity might suggest they are grog

fragments, although they may be clay pellets (size < 0.24 mm, mode = 0.112 mm in coarse fraction and size < 0.08 mm, mode = 0.032 mm in fine fraction).

The CaO concentration of MOS037 shows us that it is non-calcareous (1.64% in normalized data, Table 1 and Table 2). In XRD analysis (CER-I), no firing phases are observed (Figure 11) and the estimated EFT is below (800/850) ºC.

SEM confirms the low firing suggested by the XRD spectra. In Figure 12, the microstructure of the matrix displays initial to just less than continuous vitrification (IV-Vc-). Thus, the EFT is in the range (750-850) ºC.

3.2 Sicilian production: GR SIC

Sample FER005, from La Ferradura, is related by chemistry to the Phoenician production centre of Solunto (Sicily), and thus was labelled group SIC (Acquaro, 1998; Alaimo *et al.*, 1998). It is illustrated in thin section in Figure 13.

Group 5. Sandstone inclusions and serpentinite are the most common features of this sample. There are very rare voids, comprising common mesovughs, open-spaced, elongate with a strong alignment to the margins of sections. Some have traces of secondary calcite infilling. Elongate and equant aplastic inclusions exhibit a poor alignment to the vessel walls.

It presents an optically active, fine calcareous matrix homogeneous through the section, greyish to brown/orange in PPL and dark brown to orangish-red in XP (x25).

There is dominant sub-rounded to rounded monocrystalline quartz in the coarse fraction (size < 0.176 mm), sub-rounded to rounded calcite (size < 0.16 mm), with microfossils composed of foraminifera and mollusc fragments (size < 0.07 mm). More rarely mica-schist (size < 0.108 mm).

Tcf are dark in colour in PPL and red in XP sub-angular to sub-rounded with clear boundaries (size < 0.25 mm).

XRD analysis of this calcareous fabric (12% of CaO in normalized data, Table 1 and Table 2) (designated fabric SIC-I) suggests a low EFT, c. (800/850) ºC. It contains illite-muscovite, quartz, calcite, hematite, potassium feldspars and plagioclase (figure 14). No SEM analysis was performed because of the lack of specimen.

4. DISCUSSION

The Carthaginian imported vessels identified in this study are calcareous (CARa) to highly calcareous (CARb, CARc and CARd). They contain very well rounded quartz, along with possible indications of clay mixing and sand tempering. These technological features have been observed in the Phoenician production of Tyre (Miguel Gascón, 2014). Moreover, in the case of TFC025 (CARb), crushed calcite is used as temper, a technique also observed at the Phoenician metropolis. XRD has also revealed that most of these fabrics exhibit low EFT (below 800 ºC), similar to that of the pottery produced at Tyre (Miguel Gascón and Buxeda i Garrigós, 2013). It should be emphasized that the agreement between data from XRF and thin section petrography is not complete and that it remains to be shown whether these represent only Carthaginian products, or those of other Tunisian production centres.

The Sardinian imports, group CER, seems to be related to a different tradition especially since grog may be used as temper. Moreover, it is also a non-calcareous fabric and this lies in contrast with the technology of Carthaginian or Tyrian production.

Finally, group SIC is calcareous, low-fired (EFT below (750/800) ºC), with inclusions compatible with the geology of the Solunto area in Sicily. It presents more similarities with Tyrian ceramics than the group CER.

It is of interest that the Ilercavonia and Cossetania sites do not have amphorae from these Central Mediterranean sites, only tableware. Amongst the 220 samples examined in this study, it was clear that most of the amphorae analyzed have an Andalusian origin, especially from the areas of Málaga and Granada (Miguel Gascón, 2014). Also while the archaic Phoenician colonies in Southern Iberia produced red slip tableware and jars, none arrived in the study area. Indeed, while generally rare, the Phoenician tableware at these Northern regions is clearly from the Central Mediterranean production centres. This may indicate an important consumption preference. However, further research is needed in other sites of the early Iron Age in the Ilercavonia and Cossetania regions to confirm that pattern.

5. CONCLUSIONS

The appearance of Phoenician imports in the early Iron Age contexts of the Cossetania and Ilercavonia regions is notable not only for the first evidence of wheel-made pottery, but also in terms of the novel consumption of the products transported in these jars. This latter change in consumption and contact may have had deep social implications. The rarity of tableware in the sites studied is notable, but, when it is present, the choice of Central Mediterranean tableware and the total absence of Andalusian red slip demands explanation and clearly has meaning in socio-economic terms.

Moving to the production centres of these imported Central Mediterranean vessels, it seems that there is a clearer link between the Carthaginian products and those of Tyre, than those

produced in Sardinia and Sicily. However, clearly such judgements on the nature and cultural context of production at these centres require larger sample numbers and the detailed study of production technology in the source assemblages in Tunisia, Sicily and Sardinia.

ACKNOWLEDGEMENTS

This study was possible by David Garcia i Rubert, through his generous permission to study the materials of Sant Jaume – Mas d'en Serrà and La Ferradura and by Rafel Jornet Niella, David Asensio Vilaró, Jordi Morer de Llorens and Daniel López Reyes who allowed us to include the samples from Turó de la Font de la Canya in this study.

The XRF, XRD and SEM analyses presented were carried out in the Centres Científics i Tecnològics of the Universitat de Barcelona. The petrographic analyses were carried out at the Department of Archaeology, University of Sheffield.

Eva Miguel Gascón is indebted to the JAE-Predoc programme funded by the CSIC.

REFERENCES

Acquaro, E. (1998) Industria ceramica e archeologia della produzione nel mondo fenicio e punico nel Mediterraneo: il contributo delle analisi archeometriche. Acquaro, E. and Fabbri, B. (dris.) *Produzione e circolacione della ceramica fenicia e punica nel Mediterraneo: il contributo delle analisi archeometriche. Atti della 2ª Giornata di Archeometria della Ceramica – Ravenna, 14 maggio 1998 Giornatta Archeometria della Ceramica*, University Press Bologna, Bologna, 95-108.

Aitchison, J. (1986) *The Statistical Analysis of Compositional Data*. Chapman and Hall, London.

Aitchison, J. (2005) A concise guide to compositional data analysis. *2nd Compositional Data Analysis Workshop – CoDaWork'05*. Universitat de Girona, Girona. http://ima.udg.edu/Activitats/CoDaWork05/A_concise_guide_to_compositional_data_analysis-pdf.

Alaimo, R., Greco, C., Ilipoulos, I. and Montana, G. (2002) Phoenician-punic ceramic workshops in western Sicily: compositional characterisation of raw materials and artefacts. Kilikoglou, V., Hein, A., Maniatis, Y. (dirs.) *Modern Trends in Scientific Studies on Ancient Ceramics*, BAR International Series 1011, Oxford, 207-218.

Alaimo, R., Greco, C. and Montana, G. (1998) Le officine ceramice di Solunto: evidenza archeologica ed indagini archeometriche preliminari. Acquaro, E. and Fabbri, B. (dirs.) *Produzione e circolazione della ceramica fenicia e punica nel Mediterraneo: il contributo delle analisi archeolmetriche*. University Press Bologna, Imolla, 7-26.

Amadori, M. L. and Fabbri, B. (1998a) Indagini archeometriche su ceramica fenicia da mensa proveniente da Cartagine (VIII-VI sec. a. C.). Acquaro, E. and Fabbri, B. (dris.) *Produzione e circolacione della ceramica fenicia e punica nel Mediterraneo: il contributo delle analisi archeometriche. Atti della 2ª Giornata di Archeometria della Ceramica – Ravenna, 14 maggio 1998 Giornatta Archeometria della Ceramica*, University Press Bologna, Bologna, 43-56.

Amadori, M. L. and Fabbri, B. (1998b) Produzione locale e importazioni di ceramiche fenicie da mensa (fine VIII – fine VII secolo a. C.) a Toscanos (Spagna meridionale). Acquaro, E. and Fabbri, B. (dirs.) *Produzione e circolacione della ceramica fenicia e punica nel Mediterraneo: il contributo delle analisi archeometriche. Atti della 2ª Giornata di Archeometria della Ceramica – Ravenna, 14 maggio 1998 Giornatta Archeometria della Ceramica*, University Press Bologna, Bologna, 85-84.

Amadori, M. L. and Fabbri, B. (1998c) Studio archeometrico di ceramica fenicia (VIII-VI secolo a. C.) proveniente da siti archeologici della Sardegna e Ischia. Acquaro, E. and Fabbri, B. (dirs.) *Produzione e circolacione della ceramica fenicia e punica nel Mediterraneo: il contributo delle analisi archeometriche. Atti della 2ª Giornata di Archeometria della Ceramica – Ravenna, 14 maggio 1998 Giornatta Archeometria della Ceramica*, University Press Bologna, Bologna, 68-84.

Asensio, D., Cela, X. and Morer, J. (2005) El jaciment protohistòric del Turó de la Font de la Canya (Avinyonet del Penedès, Alt Penedès): un nucli d'acumulació d'excedents agrícoles a la Cossetània (segle VII-III aC). *Fonaments*, 12, 177-196.

Aubet, M. E. (2009) *Tiro y las colonias fenicias de Occidente*, Bellaterra, Barcelona.

Barceló-Vidal, C., Martín-Fernández, J. A. and Pawlowsky-Glahn, V. (2001) Mathematical foundations of compositional data analysis, Ross, G. (ed.) *Proceedings of IAMG'01 – The Annual Meeting of the International Association for Mathematical Geology*, *6-12 September 2001*, Cancún, México, 1-20.

Buxeda i Garrigós, J. (1999) Alteration and contamination of archaeological ceramics: the perturbation problem. *Journal of Archaeological Science*, 26, 295-313.

Buxeda i Garrigós, J. (2008) Revisiting the compositional data. Some fundamental questions and new prospects in archaeometry and archaeology. Daunis-i-Estadella, J. and Martín-Fernández, J. (eds.), *Proceedings of CODAWORK'08, the 3rd Compositional Data Analysis Workshop, May 27-30*, Universitat de Girona, Girona, 1-18.

Buxeda i Garrigós, J.; Cau, M. A.; Gurt, J. M. and Tuset, F. (1995) Análisis tradicional y análisis arqueométrico de las cerámicas communes de la época romana, *Ceràmica comuna romana d'època alto-imperial a la Península Ibèrica. Estat de la qüestió*, Monografies Emporitanes, VIII, 39-60.

455 Buxeda i Garrigós, J. and Kilikoglou, V. (2003) Total variation as a measure of variability in
456 chemical data sets. Van Zelst, L., Bishop, R. L. and Henderson, J. (dirs.) *Patterns and*
457 *Process*, Smithsonian Center for Materials Research and Education, Suitland,
458 Maryland, 18-198.
459 Cardell, C. (1999) Arqueometría de las cerámicas fenicias. Aubet, M. E., Carmona, P., Curià,
460 E., Delgado, A., Fernández, A. and Párraga, M. (dirs.) *Cerro del Villar – I. El*
461 *asentamiento fenicio en la desembocadura del río Guadalhorce y su interacción con*
462 *el hinterland*. Junta de Andalucía, Sevilla, cap. CD Anexo, 1-23.
463 Cau Ontiveros, M. A., Day, P. M. and Montana, G. (2002) Secondary calcite in archaeological
464 ceramics: Evaluation of alteration and contamination processes by thin section study.
465 Kilikoglou, V., Maniatis, Y. and Hein, A. (eds.) *Modern trends in ancient ceramics*.
466 BAR International Series 1011, Oxford, 9 – 18.
467 Garcia, D. (2009) Els sistemes de fortificació de la porta d'accés a l'assentament de la primera
468 edat del ferro de Sant Jaume (Alcanar, Montsià), *Revista d'Arqueologia de Ponent*,
469 19, 205-229.
470 Garcia, D. and Gracia, F. (2011) Phoenician trade in the north-east of the Iberian Peninsula: a
471 Historiographical problem. *Oxford Journal of Archaeology*, 30(1), 33-56.
472 Garcia, D., Moreno, I., Gracia, F., Font, L. and Mateu, M. (2015) Genesis and Development of
473 the First Complex Societies in the Northeastern Iberian Peninsula During the First
474 Iron Age (7^{th}- 6^{th} Centuries BC). The Sant Jaume Complex (Alcanar, Catalonia),
475 Militello, P. M. and Öniz, H. (eds.) *SOMA 2011*, BAR International Series 2695 (I),
476 Oxford, 445-452.
477 Kilikoglou, V. (1994) Scanning Electron Microscopy. Wilson, D.E. and Day, P.M., Ceramic
478 Regionalism in Prepalatial Central Crete: The Mesara Imports at EMI to EMIIA
479 Knossos, *Annual of the British School at Athens*, 89, 1-87.
480 Maluquer, J. (1983) *El poblado ibérico de La Ferradura , Ulldecona (Tarragona)*. P. I. P. VII,
481 CSIC – Universitat de Barcelona, Barcelona.
482 Miguel Gascón, E. and Buxeda i Garrigós, J. (2013) Characterization of possible Phoenician
483 pottery production of Tyre. *Applied Clay Science*, 82, 79-85.
484 Miguel Gascón, E. (2014) *El comercio fenicio arcaico en la Ilercavonia y la Cossetania.*
485 *Proveniencia y tecnología del material cerámico en un contexto colonial del oeste*
486 *mediterráneo*, Doctoral Thesis, Universidad de Zaragoza.
487 Pradell, T., Martín, M., García-Vallés, M. and Vendrell-Saz, M. (1995) Attribution of "painted
488 Iberian" and "monochrome grey Greek" ceramics of the 6^{th} century B. C. to a local
489 production of Ullastret (Catalonia). Vendrell-Saz, M., Molera, M., García-Vallés, M.
490 (dirs.) *Estudis sobre cerámica antiga*. Departament de Cultura, Generalitat de
491 Catalunya, Barcelona, 23-27.

R Core Team (2013) *R: A language and environment for statistical computing*. R Foundation for Statistical Computing, Vienna, Austria.

Rafel, N. (2013) La Cuenca minera del Baix Priorat (Tarragona): explotación y distribución en época colonial. Recursos locales versus recrusos alóctonos. Aubet, M. E. and Sureda, P. (dirs.), *Interacción social y comercio en la antesala del colonialismo. Actas del Seminario Internacional celebrado en la Universidad Pompeu Fabra el 28 y 29 de marzo de 2012*, Publicaciones del Laboratorio de arqeuología de la Universidad Pompeu Fabra de Barcelona, Barcelona, Cuadernos de Arqueología Mediterránea, 21, 71-85.

Vendrell-Saz, M. (2005) Anàlisi de les ceràmiques i mostres de forns d'època grega arcaica de Sant Martí d'Empúries. *Ceràmiques jònies d'època arcaica: centre de producció i comercialització al Mediterrani Occidental*, Monografies Emporitanes, Museu d'Arqueologia de Catalunya, Barcelona, 11, 339-346.

Whitbread, I. K. (1989) A proposal for the systematic description of thin sections towards the study of ancient technology. Maniatis, Y. (dir.), *Archaeometry Proceedings of the 25th International Symposium (held in Athens form 19 to 23 May 1986)*, Elsevier, Amsterdam, 127-138.

Whitbread, I. K. (1995) *Greek Transport Amphorae. A Petrological and Archaeological Studi*. Fitch Laboratory Occasional Paper, 4, British School at Athens, Athens.

Whitney, D. L. and Evans, B. W. (2010) Abbreviations for names of rock-forming minerals. *American Mineralogist*, 95, 185-187.

Table 1

	MOS026	MOS040	MOS060	MOS037	FER005	TFC025	TFC036	TFC040	TFC041	TFC072
Fe_2O_3 %	5.06	5.02	5.04	4.30	6.88	5.09	4.89	4.83	4.97	5.47
Al_2O_3 %	12.26	13.99	13.76	19.66	17.63	14.03	12.49	14.58	14.61	16.38
MnO %	0.03	0.03	0.03	0.05	0.08	0.06	0.04	0.03	0.05	0.02
P_2O_5 %	0.22	0.24	0.21	0.11	0.23	0.48	0.29	0.45	0.39	0.47
TiO_2 %	0.61	0.87	0.88	0.74	0.80	0.74	0.63	0.79	0.81	0.88
MgO %	1.85	1.63	1.62	1.39	1.66	1.59	1.48	1.40	1.39	2.15
CaO %	19.49	9.62	9.57	1.64	12.03	21.47	18.05	17.49	18.24	26.15
Na_2O %	0.43	0.63	0.77	1.92	0.63	0.42	0.43	0.43	0.39	0.87
K_2O %	1.32	2.40	2.40	4.41	2.27	2.41	1.40	2.67	2.60	1.83
SiO_2 %	58.60	65.41	65.54	65.61	57.64	53.39	60.11	57.05	56.33	45.48
Ba (ppm)	171	544	584	514	516	2105	591	1463	1274	1460
Rb (ppm)	57	95	96	182	94	109	54	116	117	87
Th (ppm)	9	12	9	27	10	12	4	11	12	11
Nb (ppm)	18	20	18	21	18	17	16	18	19	19
Pb (ppm)	21	17	23	77	39	27	23	29	29	29
Zr (ppm)	156	291	288	189	183	213	169	227	222	180
Y (ppm)	19	30	32	46	30	31	20	31	32	35
Sr (ppm)	460	206	206	131	236	382	493	317	299	675
Ce (ppm)	58	82	69	121	69	76	60	73	71	83
Ga (ppm)	19	14	14	26	17	17	16	17	18	21
V (ppm)	93	83	88	105	108	99	123	102	105	98
Zn (ppm)	95	78	63	121	82	78	94	71	69	144
Cu (ppm)	15	16	16	39	19	19	16	39	26	36
Ni (ppm)	31	31	30	26	51	30	31	29	30	61
Cr (ppm)	85	95	85	71	101	59	98	63	62	142

Table 2

	CARa (n = 2)		CARb (n = 3)		CARc (n = 1)	CARd (n = 2)		CER (n = 1)	SIC (n = 1)
	m	sd	m	sd		m	sd		
Fe_2O_3 %	5.03	0.01	4.96	0.13	5.47	4.97	0.12	4.30	6.88
Al_2O_3 %	13.87	0.16	14.40	0.33	16.38	12.37	0.16	19.66	17.63
MnO %	0.03	0.00	0.05	0.01	0.02	0.04	0.01	0.05	0.08
P_2O_5 %	0.22	0.03	0.43	0.05	0.47	0.25	0.05	0.11	0.23
TiO_2 %	0.87	0.01	0.78	0.03	0.88	0.62	0.02	0.74	0.80
MgO %	1.63	0.01	1.46	0.11	2.15	1.65	0.26	1.39	1.66
CaO %	9.60	0.03	18.99	2.11	26.15	18.76	1.02	1.64	12.03
Na_2O %	0.70	0.10	0.41	0.02	0.87	0.43	0.00	1.92	0.63
K_2O %	2.40	0.01	2.56	0.14	1.83	1.36	0.06	4.41	2.27
SiO_2 %	65.48	0.09	55.57	1.94	45.48	59.35	1.07	65.61	57.64
Ba (ppm)	564	28	1577	436	0.146	318	297	514	516
Rb (ppm)	95	1	114	4	87	55	2	182	94
Th (ppm)	10	2	12	1	11	6	4	27	10
Nb (ppm)	19	1	18	1	19	17	1	21	18
Pb (ppm)	20	4	28	1	29	22	1	77	39
Zr (ppm)	289	2	221	7	180	162	9	189	183
Y (ppm)	31	1	31	1	35	19	1	46	30
Sr (ppm)	206	0	331	44	675	476	23	131	236
Ce (ppm)	75	9	73	3	83	59	1	121	69
Ga (ppm)	14	0	17	1	21	17	2	26	17
V (ppm)	85	4	102	3	98	107	21	105	108
Zn (ppm)	70	11	73	5	144	94	1	121	82
Cu (ppm)	16	0	27	10	36	15	1	39	19
Ni (ppm)	30	1	30	1	61	31	0	26	51
Cr (ppm)	90	7	61	2	142	91	9	71	101

Figure 1

Click here to download high resolution image

Figure 2

Click here to download high resolution image

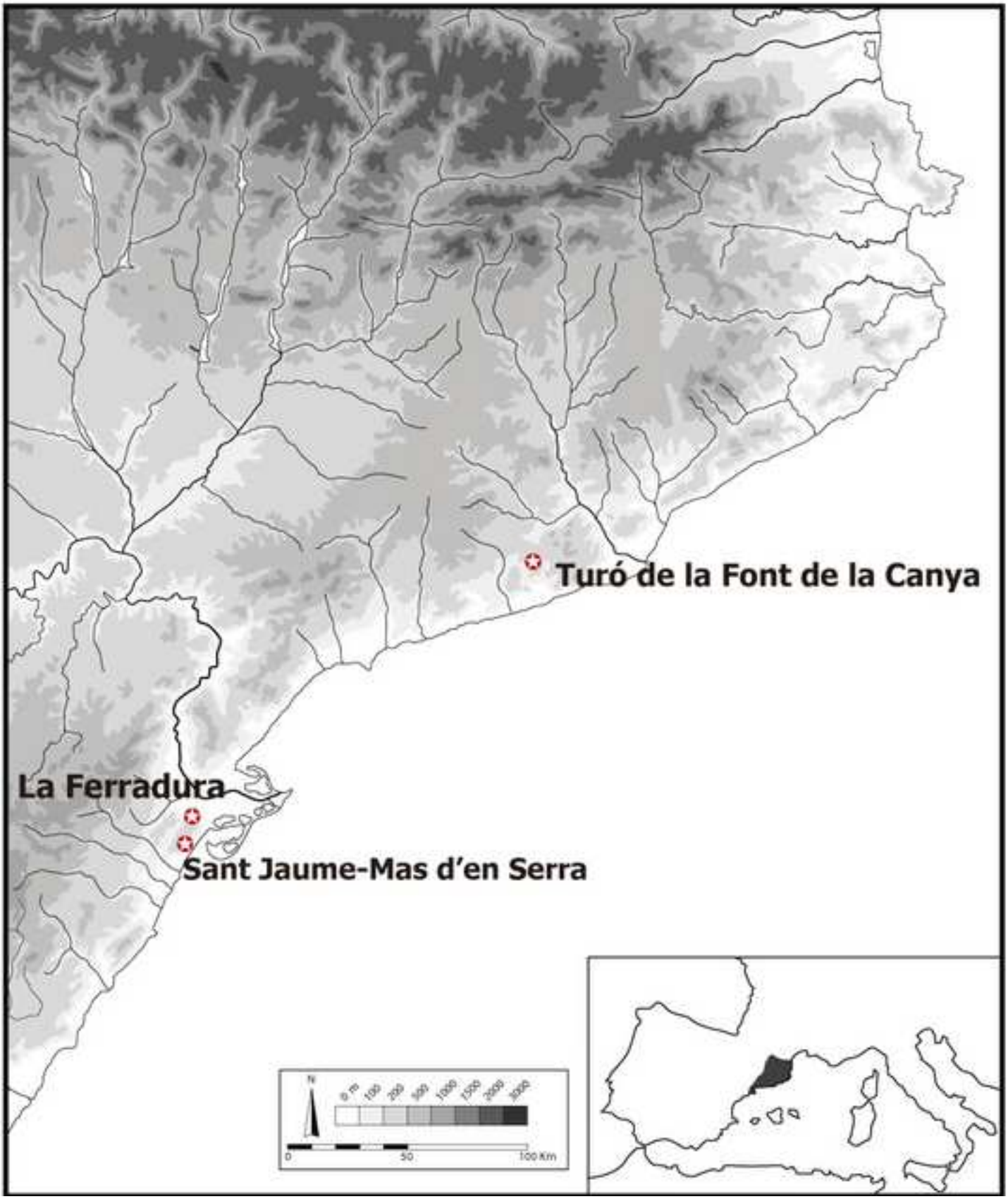

Figure 3

Click here to download high resolution image

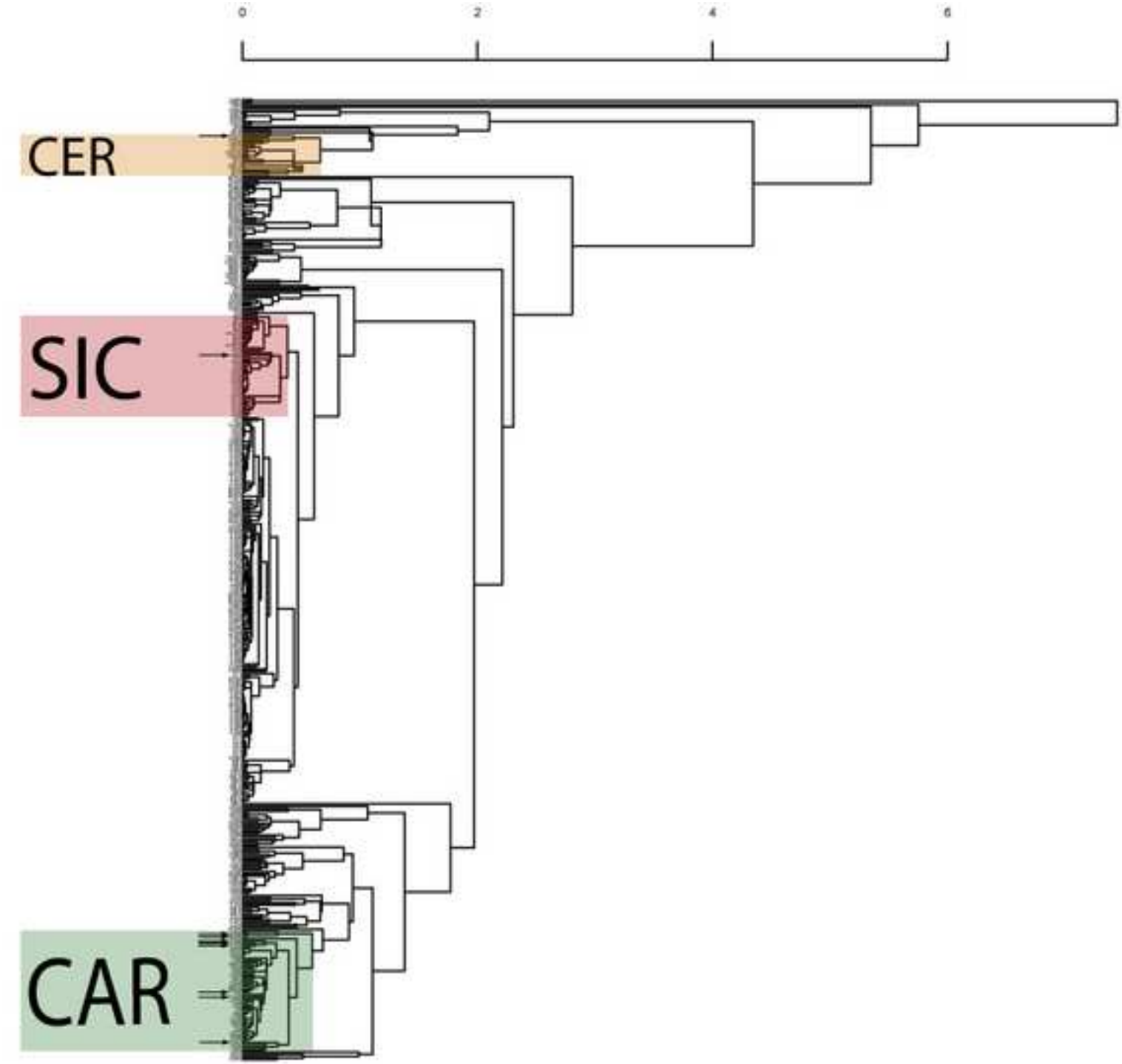

Figure 4

Click here to download high resolution image

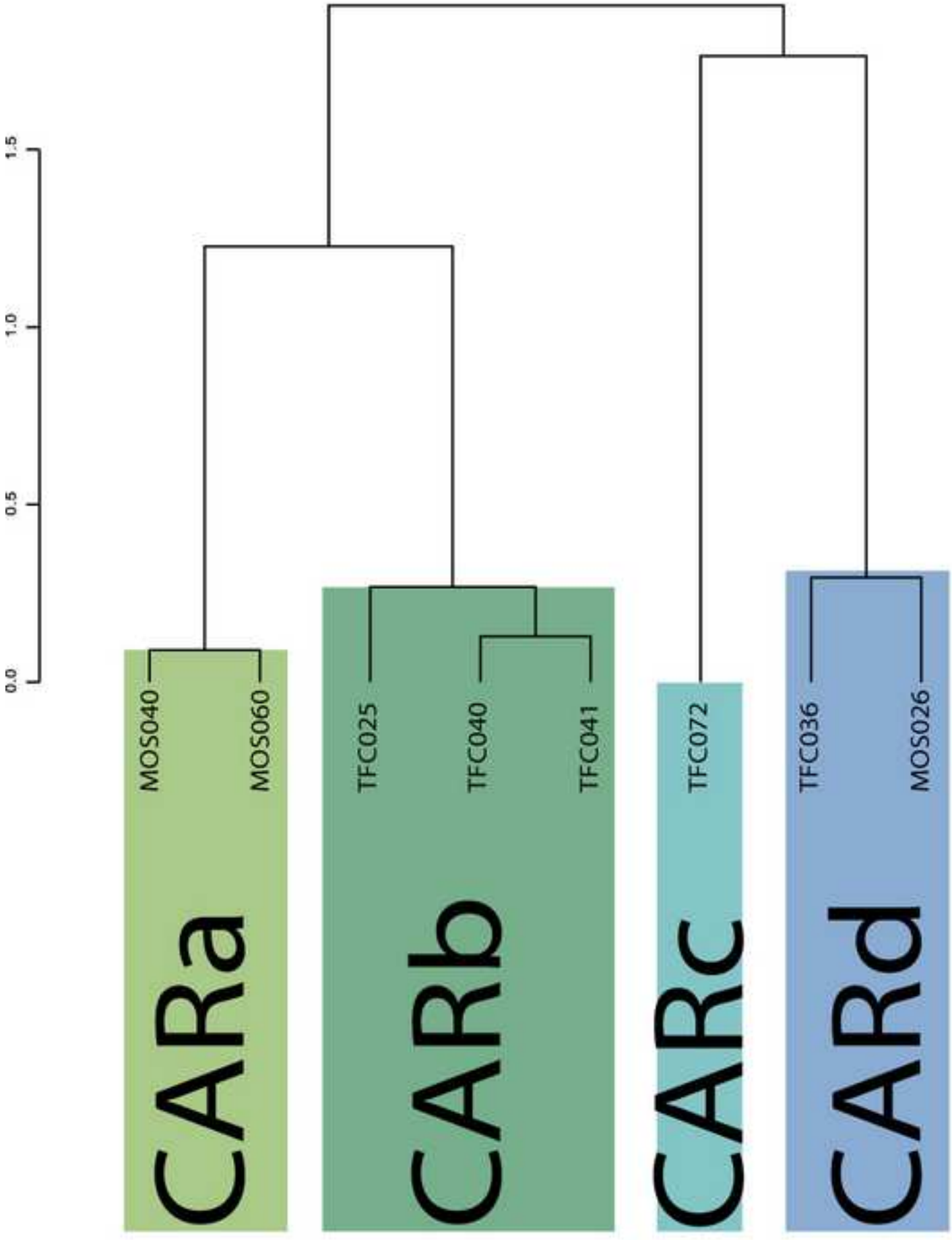

Figure 5

Click here to download high resolution image

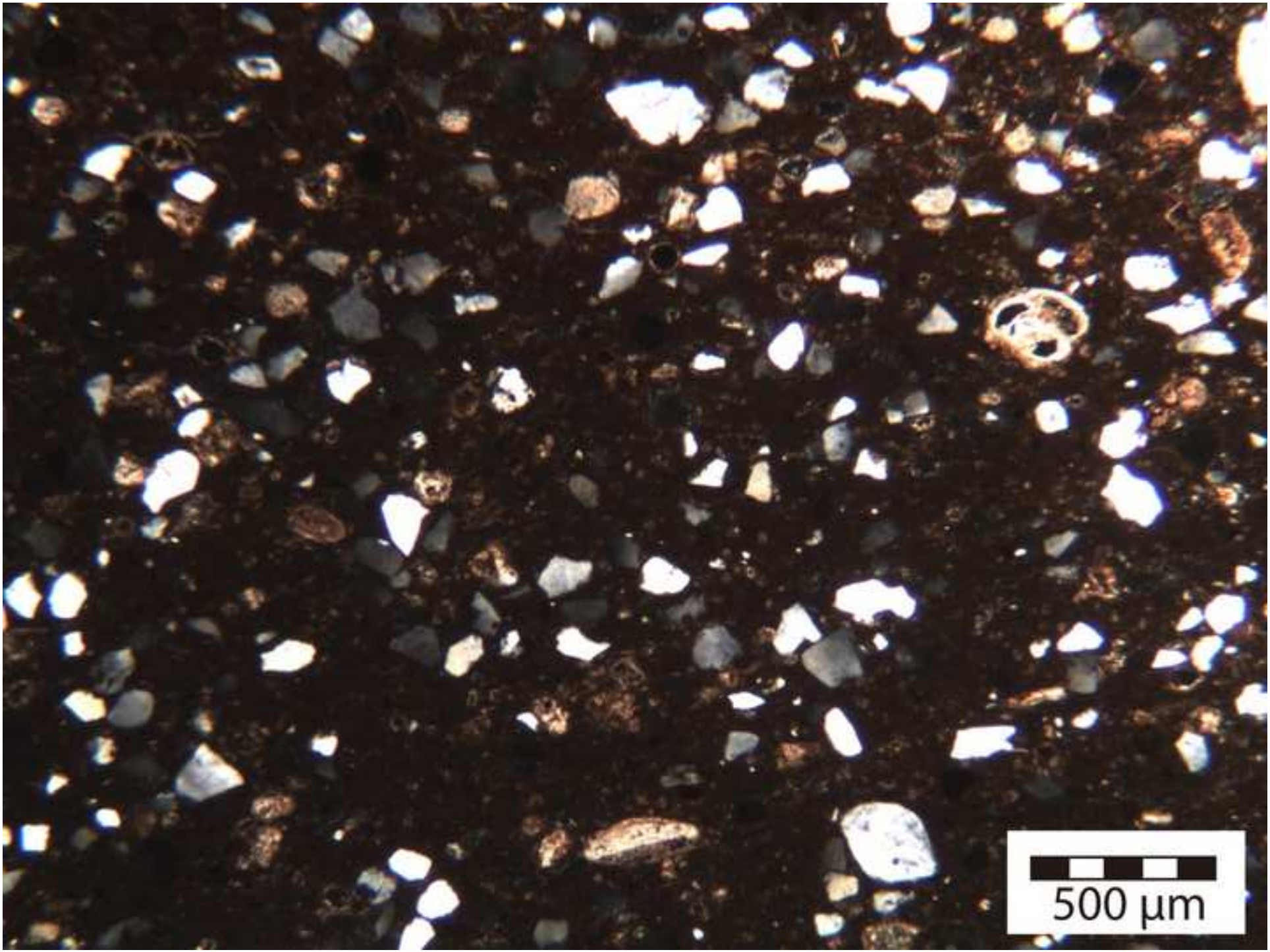

Figure 6

Click here to download high resolution image

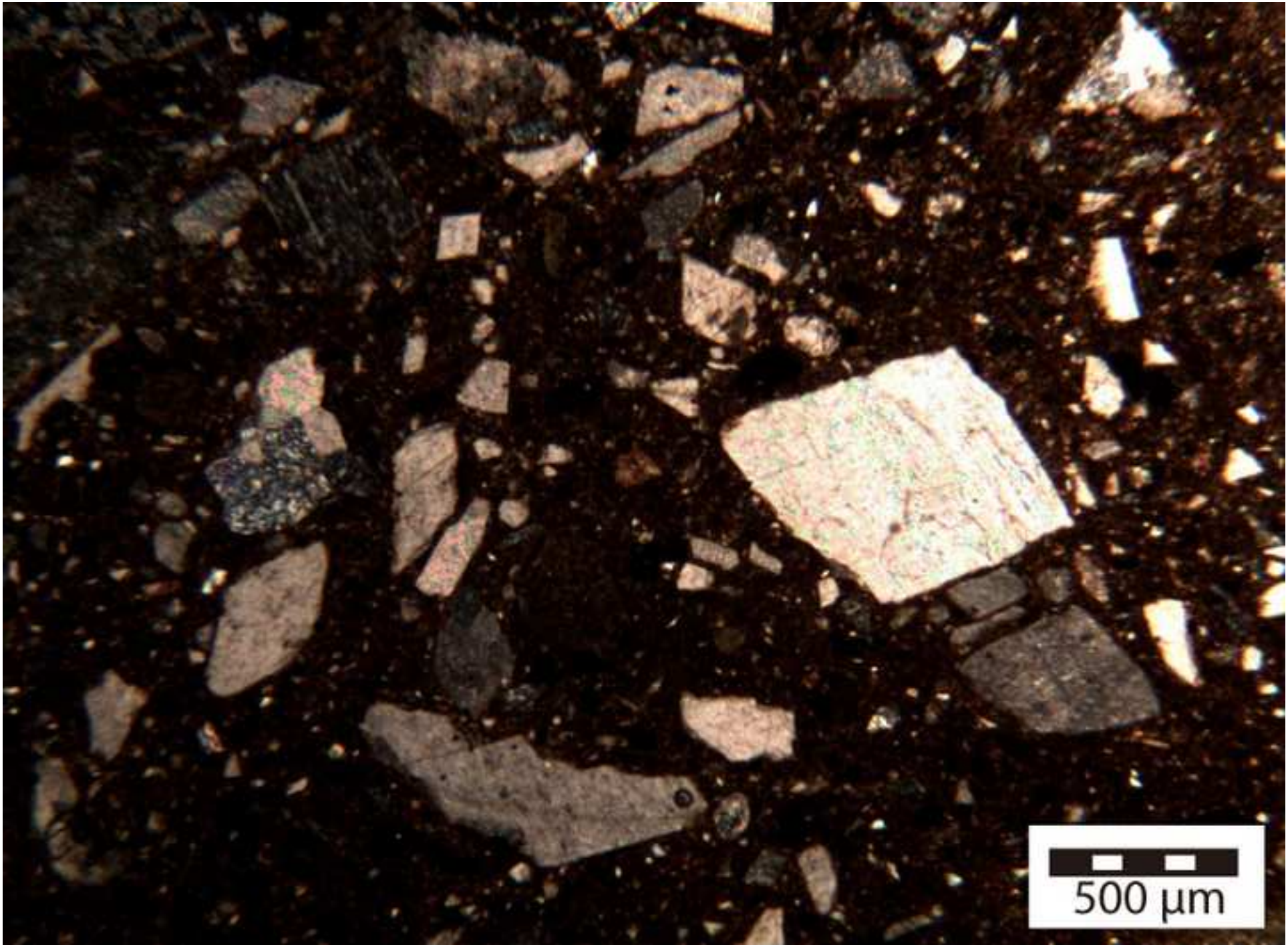

Figure 7

Click here to download high resolution image

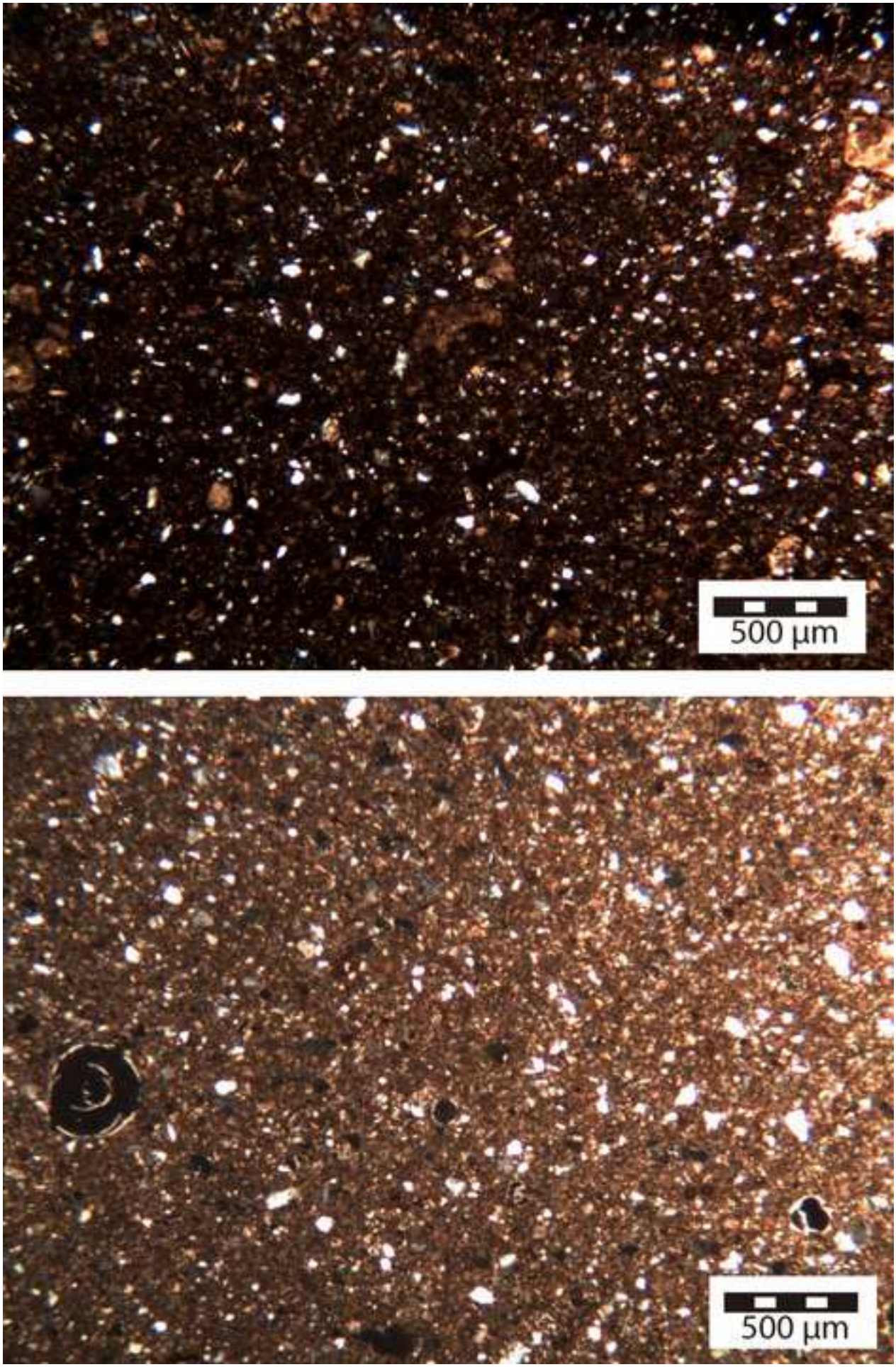

Figure 8

Click here to download high resolution image

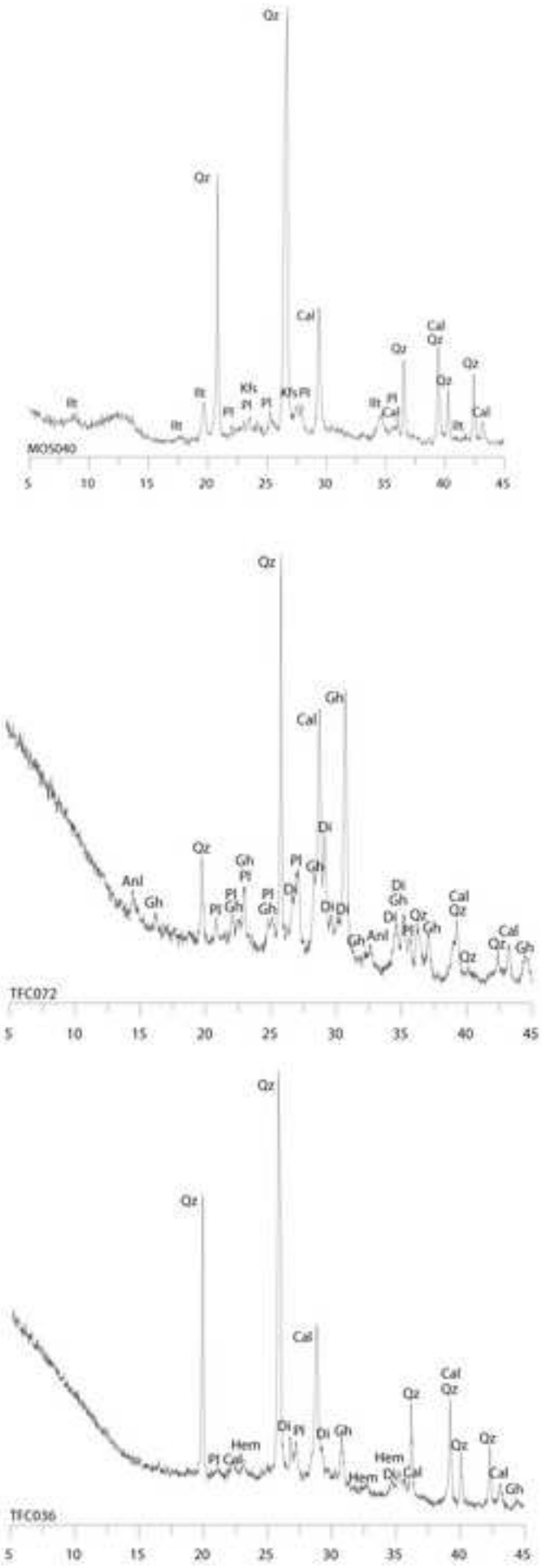

Figure 9

Click here to download high resolution image

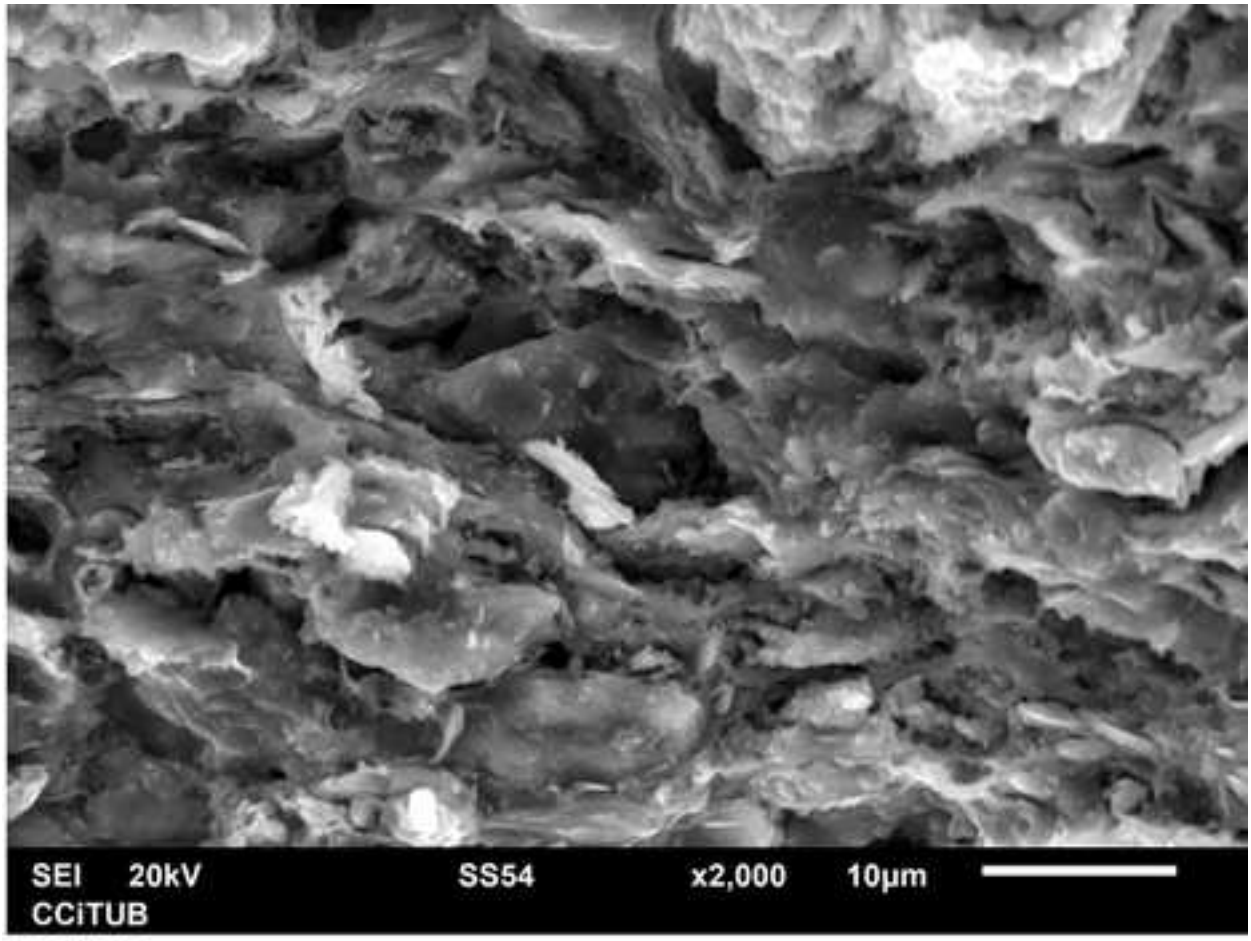

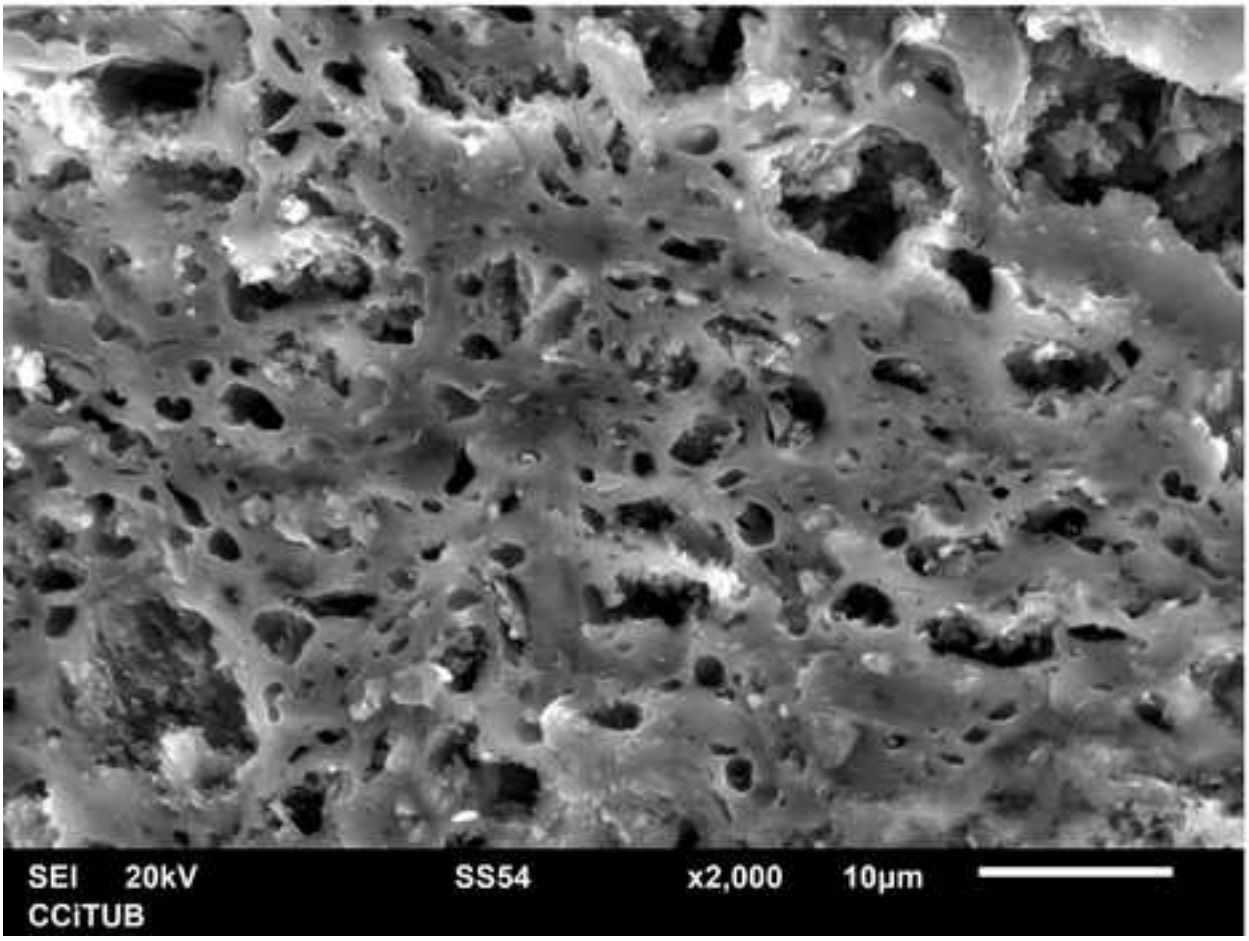

Figure 10

Click here to download high resolution image

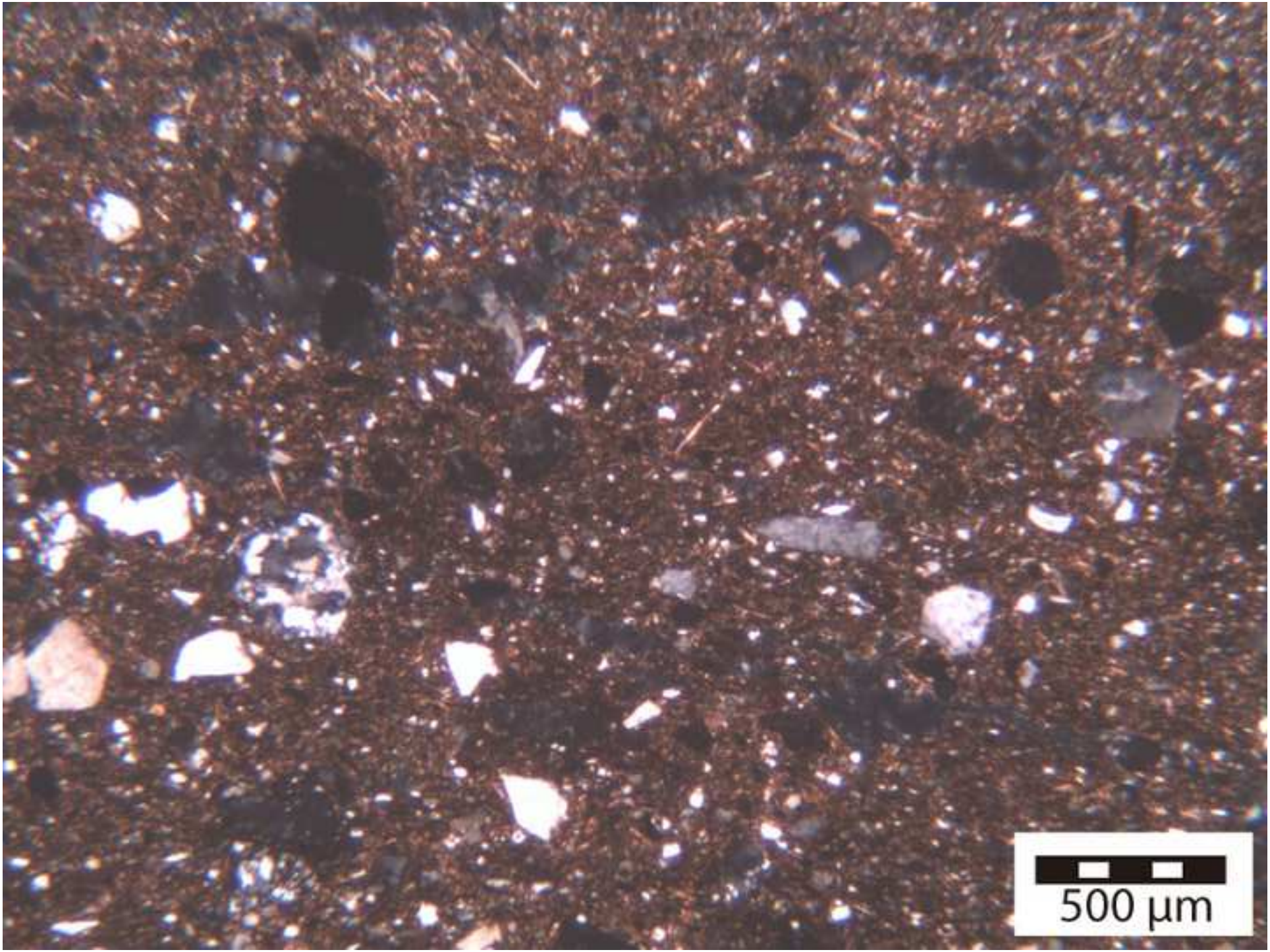

Figure 11

Click here to download high resolution image

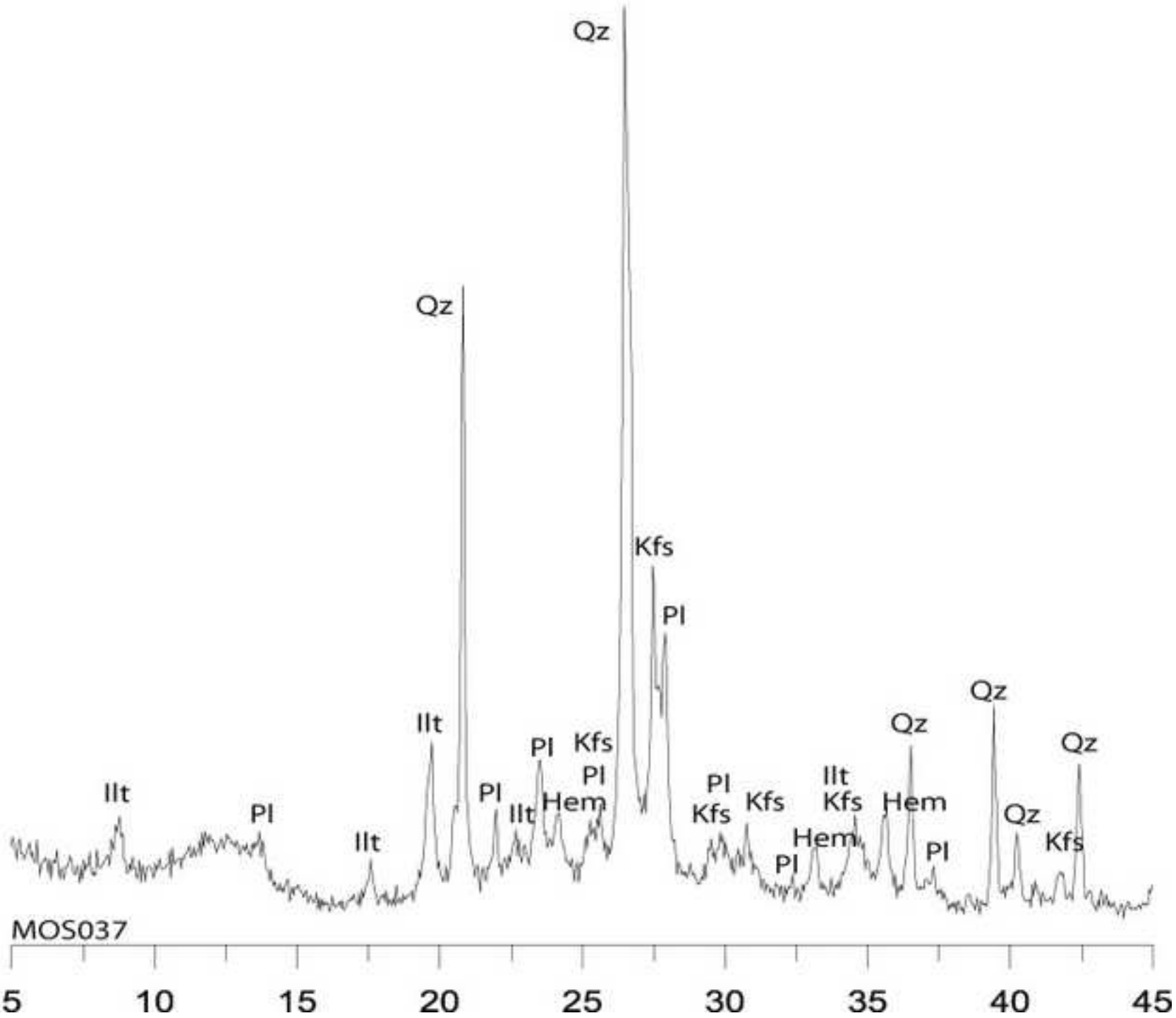

Figure 12

Click here to download high resolution image

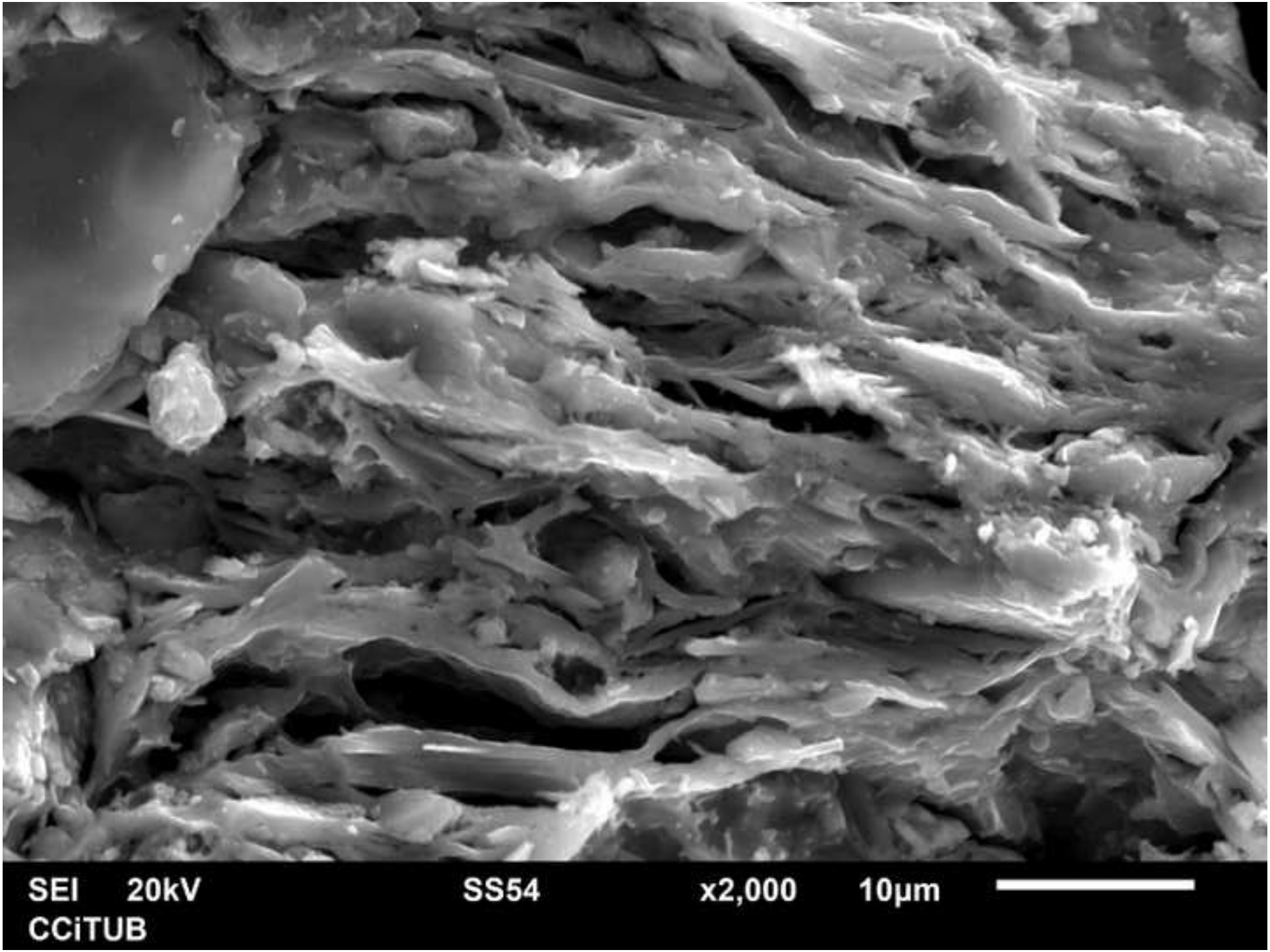

Figure 13

Click here to download high resolution image

Figure 14

Click here to download high resolution image

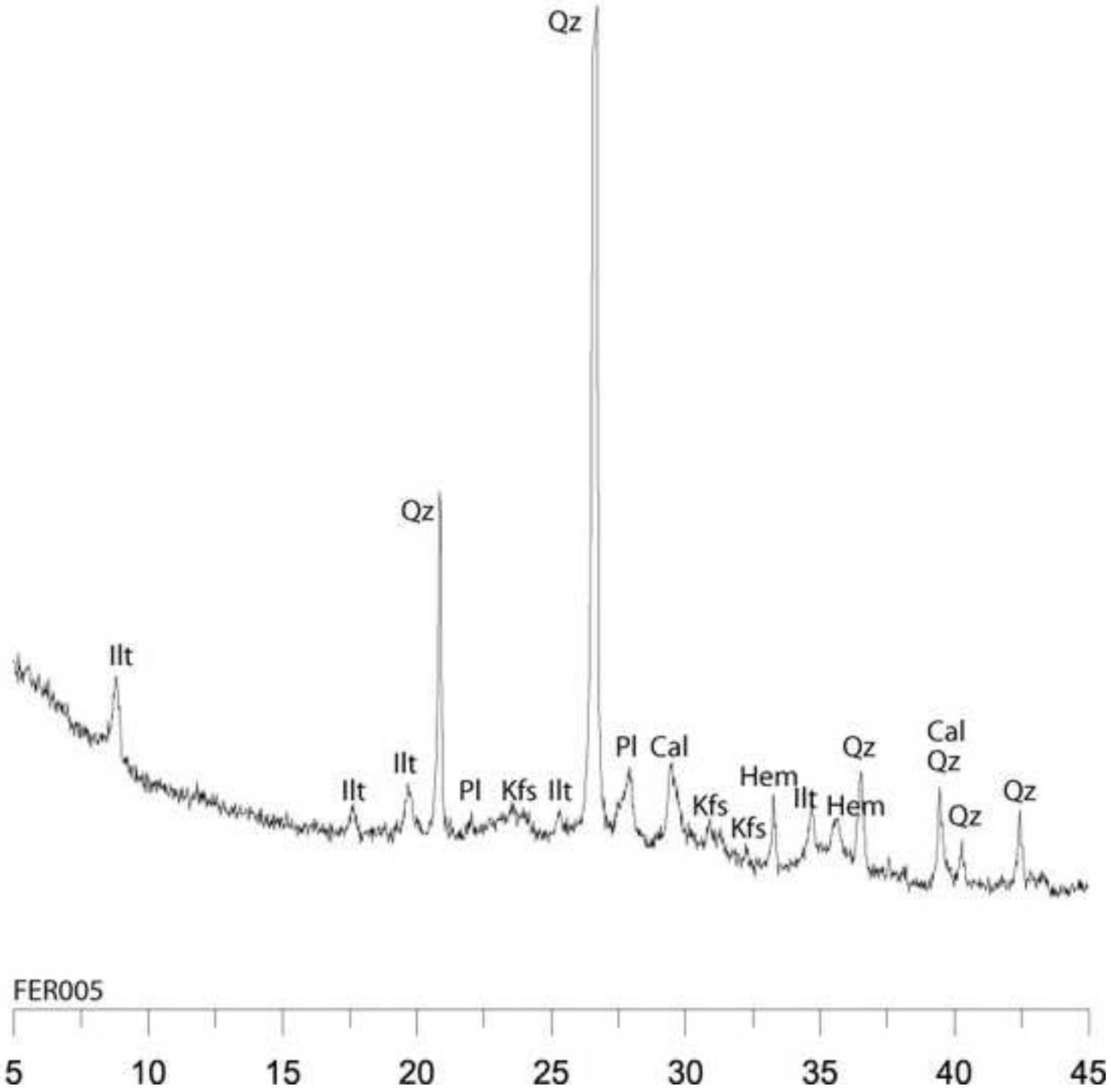

Table 1 Normalized concentrations of the chemical compositions of the analyzed samples

Table 2 Mean (m), standard deviation (sd) and normalized concentrations of the chemical composition group cited in the text

Figure 1 Western Phoenician colonies and Phoenician production centres located at the Circle of the Strait of Gibraltar

Figure 2. Location of the sites sampled where Central Mediterranean Phoenician products are found

Figure 3 Dendrogram illustrating cluster analysis of the 218 Phoenican individuals of ARQUB's database, along with the 178 published samples.

Figure 4. Dendrogram of the eight Phoenician individuals of possible Carthaginian provenance after cluster analysis.

Figure 5 Group 1: Photomicrograph, showing rounded quartz and calcite inclusions. TFC036 (fabric CARd-II) in XP (x25).

Figure 6 Group 2: Photomicrograph illustrating crushed calcite inclusions. TFC025 (fabric CARb-I) in XP (x25).

Figure 7 Group 3: Photomicrographs showing allotriomorphic quartz and mica matrix. TFC041 (fabric CARb-I) in XP (upper) and MOS040 (fabric CARa-I) in XP (lower)(x25)

Figure 8 XRD spectra. Top: MOS040, fabric CARa-I. Centre: TFC072, fabric CARc-I. Bottom: TFC036, fabric CARd-II. Cal: calcite; Qz: quartz; Ilt: illite-moscovite; Pl: plagioclase; Gh: gehlenite; Di: diopside (pyroxene); Hem: hematite; Anl: analcime. Abbreviations after Whitney and Evans (2010).

Figure 9 SEM microphotographs. Top: TFC041 (fabric CARb-I). Bottom: TFC036 (fabric CARd-II)

Figure 10 Group 4: Photomicrograph illustrating extural concentration features/grog temper. MOS037 (fabric CER-I) in XP (x25)

Figure 11 XRD spectrum. MOS037 (fabric CER-I). Qz: quartz; Ilt: illite-moscovite; Pl: plagioclase

Figure 12 SEM photomicrograph of MOS037 (fabric CER-I)

Figure 13 Group 5: Photomicrograph showing sandstone inclusions and serpentinite. FER005 (fabric SIC-I) in XP (x25)

Figure 14 XRD spectrum of FER005 (FabricSIC-I). Qz: quartz; Ilt: illite-muscovite; Pl: plagioclase; Hem: hematite; Kfs: potassium feldspars.